MAJIS/JUICE VIS-NIR FM and SM detectors characterization

Cisneros-González, Miriam, Bolsée, David, Pereira, Nuno, Van Laeken, Lionel, Depiesse, Cédric, et al.

Miriam Cisneros-González, David Bolsée, Nuno Pereira, Lionel Van Laeken, Cédric Depiesse, Lars Jacobs, Séverine Robert, Ann C. Vandaele, Samuel Gissot, Özgür Karatekin, François Poulet, Yves Langevin, Cydalise Dumesnil, Jean Pierre Dubois, Antoine Arondel, Paolo Haffoud, Christian Ketchazo, Veronique Hervier, Bruno Crane, "MAJIS/JUICE VIS-NIR FM and SM detectors characterization," Proc. SPIE 11443, Space Telescopes and Instrumentation 2020: Optical, Infrared, and Millimeter Wave, 114431L (13 December 2020); doi: 10.1117/12.2562063

SPIE.

Event: SPIE Astronomical Telescopes + Instrumentation, 2020, Online Only

MAJIS/JUICE VIS-NIR FM and SM detectors characterization

Miriam E. Cisneros-González[a], David Bolsée[b], Nuno Pereira[b], Lionel Van Laeken[b], Cédric Depiesse[b], Lars Jacobs[b], Séverine Robert[a,b], Ann C. Vandaele[b], Samuel Gissot[c], Özgür Karatekin[c], François Poulet[d], Yves Langevin[d], Cydalise Dumesnil[d], Jean Pierre Dubois[d], Antoine Arondel[d], Paolo Haffoud[d], Christian Ketchazo[d], Veronique Hervier[d], and Bruno Crane[d]

[a]Institute of Condensed Matter and Nanosciences, Université catholique de Louvain, B-1348 Louvain-la-Neuve, Belgium
[b]Royal Belgian Institute for Space Aeronomy (BIRA-IASB), 1180 Brussels, Belgium
[c]Royal Observatory of Belgium (ROB), 1180 Brussels, Belgium
[d]Institute of Space Astrophysics (IAS), 91440 Bures-sur-Yvette, France

ABSTRACT

MAJIS (Moons And Jupiter Imaging Spectrometer) is one of the science instruments of the ESA L-Class mission JUICE (Jupiter ICy Moons Explorer) to be launched in 2022 with an arrival at Jupiter in 2030. MAJIS will perform imaging spectroscopy through two channels: VIS-NIR (0.50 μm - 2.35 μm) and IR (2.25 μm - 5.54 μm). The Royal Belgian Institute for Space Aeronomy (BIRA-IASB) and the Royal Observatory of Belgium (ROB) contribute to MAJIS with the characterization of the VIS-NIR Flight Model (FM) and Spare Model (SM) detectors, including the design, development and validation of the setup, and the data processing pipeline. Typical detector characterization measurements were performed during the campaigns but also calibrated measurements such as Quantum Efficiency (QE). Since some of the characterization measurements require different illumination conditions, temperature, beam uniformity, exposure time, and/or data acquisition procedure, the characterization setup is configurable for dark conditions, uniform light beam, and convergent beam with same focal ratio as MAJIS convergence optics. The thermal-vacuum characterization facility was completed at BIRA-IASB premises and was subjected to validation tests on late 2019 and early 2020. MAJIS VIS-NIR FM detector was delivered for its complete characterization in June 2020; SM characterization shall be performed after time of meeting. In this paper, we summarize the optical and thermal performances of the facility, the detector's mechanical integration method and its optical alignment into the setup, the security system implemented, the general operation of the setup during the characterization campaign, and FM preliminary result analyses.

Keywords: JUICE, MAJIS, VIS-NIR detectors, detectors characterization, imaging spectroscopy, cryogenic temperatures, dark current, linearity

1. INTRODUCTION

MAJIS (Moons And Jupiter Imaging Spectrometer) is one of the science instruments of the ESA L-Class mission JUICE (Jupiter ICy Moons Explorer), to be launched in 2022 and arrival at Jupiter in 2030. MAJIS will perform detailed observations of the Jovian System, including Jupiter and the Galilean satellites. MAJIS is intended to: 1) study the composition and physical properties of the surfaces of the satellites, 2) characterize its exospheres, 3) study the atmosphere of Jupiter at different levels (including auroras, magnetic footprints and hotspots), 4) characterize the whole Jovian system (including ring system, dust and small inner moons), and 5) monitor particular aspects of the satellites (including Io and Europa torii and Io's volcanic activity)[1].

Further author information:
M.C.: E-mail: miriam.cisneros@uclouvain.be, Telephone: +32 (0)2 373 03 50
D.B.: E-mail: david.bolsee@aeronomie.be, Telephone: +32 (0)2 373 03 51

Space Telescopes and Instrumentation 2020: Optical, Infrared, and Millimeter Wave, edited by Makenzie Lystrup, Marshall D. Perrin, Proc. of SPIE Vol. 11443, 114431L · © 2020 SPIE
CCC code: 0277-786X/20/$21 · doi: 10.1117/12.2562063

MAJIS combines two different spectral channels: VIS-NIR (0.5 μm - 2.35 μm), and IR (2.25 μm - 5.54 μm)[2]. The MAJIS VIS-NIR detector must be radiometrically characterized before being integrated on the spacecraft to ensure a proper data processing of the signals that will be collected by the instrument during the mission[3]. In this way, it will be possible to verify and validate the performances of the detectors within the in-flight operation, by reproducing high-vacuum and cryogenic conditions in a safe controlled environment. The Royal Belgian Institute for Space Aeronomy (BIRA-IASB) and the Royal Observatory of Belgium (ROB) are in charge of the full characterization of the spare (SM) and flight models (FM) of the MAJIS VIS-NIR detectors[4]. However, the characterization campaigns were done through a close collaboration with the Institute of Space Astrophysics (IAS), who is also the lead institute of the MAJIS instrument. The project was supervised by the National Center for Space Studies (CNES), especially concerning the safety of the detectors, and by the Belgian User Support and Operations Center (B.USOC) as the Product and Quality Assurance (PA/QA) of the campaigns of measurements[5]. The facility to perform the characterization of the MAJIS VIS-NIR detectors was developed at BIRA-IASB in 2019, and fully validated on early 2020[6].

At instrument level, each detector is integrated in a mechanical enclosure, known as the Focal Plane Unit (FPU), that guarantees the nominal cleanliness, thermalization, straylight rejection and optical alignment of its internal components, including the Focal Plane Array (FPA) and the Focal Plane Electronics (FPE)[6]. To characterize the response of the MAJIS VIS-NIR detectors, it is expected to measure different properties. Depending on the type of measurement to be performed, some parameters need to be measured at different wavelengths, dynamical illumination levels, integration times, or temperatures (Figure 1). Additionally, some of the measurements need to be repeated after the integration of the high-pass Linear Variable Filter (LVF) in front of the FPA of the FM detector, as it would be the final configuration of the MAJIS VIS-NIR FPU. Therefore, the FM characterization campaign was divided in two parts: FPU without LVF (June 29^{th} - July 14^{th}, 2020), and FPU with LVF (August 24^{th} - 31^{st}, 2020). In the case of the SM detector, only the final configuration of the FPU will be characterized by mid-January 2021.

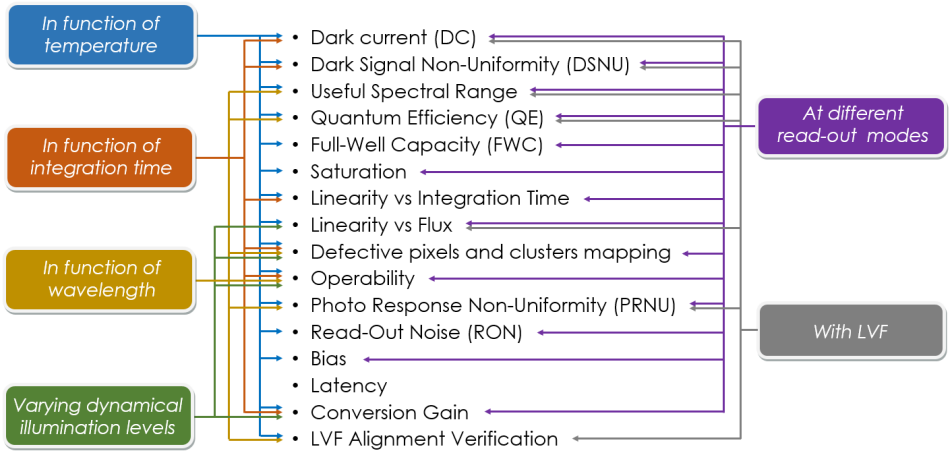

Figure 1. Parameters to be measured during the MAJIS VIS-NIR detectors characterization. The characterization facility was designed to provide a temperature range from 116 K to 160 K, a uniform monochromatic light beam tunable from 0.4 μm to 2.65 μm, and up to 30 different illumination levels. The Linear Variable Filter (LVF) will be integrated in front of the detector to repeat measurements that confirm the functionality of the VIS-NIR detector in its final configuration.

2. CHARACTERIZATION FACILITY

The opto-mechanical facility developed to characterize the MAJIS VIS-NIR detectors is constituted by three main blocks[6]:

- **Light entrance:** It produces a stable radiance with a continuum over the spectral range of the MAJIS VIS-NIR channel. Moreover, by the combination of different neutral density filters, up to 30 different

illumination levels for the detector can be provided. For latency measurements, an electronic shutter is especially included in this block.

- **Spectrometer:** It consists in a double monochromator and its electronics for phase-sensitive or unmodulated detection. The spectrometer includes its own internal filter wheel for second order rejection and an additional CLOSE position. The monochromatic beam obtained is directed to the third block through the output of the monochromator by an optical fiber.

- **Detection:** This block is constituted by a four-ports integrating sphere and a high-vacuum chamber, within which the detector can be thermalized at temperatures between 116 K and 160 K. Calibrated PbS or Si detectors in the integrating sphere are used to perform calibrated measurements, such as Quantum Efficiency (QE).

The facility provides a light beam in the wavelength range of 0.4 μm - 2.65 μm to perform several characterization measurements at different temperatures[6]. The stability of the lamp at the entrance block is continuously monitored by a multi-channels filter radiometer, although only the four channels with the largest central wavelengths (613.03 nm, 671.98 nm, 869.10 nm and 940.70 nm) were used during the MAJIS VIS-NIR FM characterization campaign. Additionally, the facility provides an uncalibrated PbS or Si detector at the dual output of the monochromator for additional monitoring when the direct signal needs to be known before the attenuation by the fiber and the integration sphere. However, the main reference signal for the characterization comes from the calibrated detectors at the integrating sphere which is complemented by an InGaAs detector also available at the integrating sphere. The InGaAs detector covers the whole VIS-NIR spectral range of the facility, while the Si detector needs to be replaced by the PbS detector above 1 μm.

It is worth mentioning that the optical system outside the vacuum chamber can be continuously flushed with nitrogen to remove the water vapor absorption in the NIR wavelength range. Both the optical bench and the vacuum chamber are located in an ISO-5 area where the detector can be exposed without risk of particle contamination (up to 54 ppm)[7].

Inside the vacuum chamber, the detector is surrounded by a radiation shield that remains at a stable temperature below 172 K and includes a movable Short Wave Pass Filter (SWPF) to remove the background thermal emission coming from both the window of the vacuum chamber and the integrating sphere[6]. Both the radiation shield and the FPU are supported by a special designed mount that additionally centers the field of view of the detector in front of the viewport of the vacuum chamber. As demanded by IAS[7], no thermometry device nor heater of the FPU was used for thermal control, but only for temperature monitoring. The thermalization of the detector (and other components of the FPU mount) was possible thanks to a closed cycle cryocooler and two PID control loops (one redundant), constituted by calibrated temperature sensors and heaters located at the copper base plate that supports the FPU[6]. Thanks to its integrated security system,[8] the facility ensures the safety of the internal components of the FPU in a high-vacuum level environment that operates below 10^{-5} mbar with a molecular cleanliness level of 5×10^{-7} g/cm^2 and free of iced water contamination, even during unexpected events. The temperature and vacuum conditions of the FPU and other relevant components inside the vacuum chamber are continuously monitored by the Thermal Ground Support Equipment (TGSE) system, accessible to the operators from the control room.

The facility can also provide three different configurations to characterize the detector[6].The optical configuration 1 provides dark conditions to the detector over the whole MAJIS VIS-NIR operating range (0.5 μm - 2.35 μm) by limiting the thermal contribution and straylight from warm objects around the detector thanks to the cold movable plate in closed position and the cold radiation shield. The optical configuration 2 is used to uniformly illuminate the detector by the integrating sphere, useful for the parameters that need light conditions to be measured. Finally, the optical configuration 3 provides the appropriate light beam convergence that the detector should receive from the MAJIS collimating optics after its integration in the instrument. In this configuration, an optical focusing array constituted by two concave off-axis mirror, is added between the integrating sphere and the detector, so the measurements with the LVF installed at the FPU can be performed. Either in configuration 2 or configuration 3, the movable plate can be in OPEN or SWPF position depending

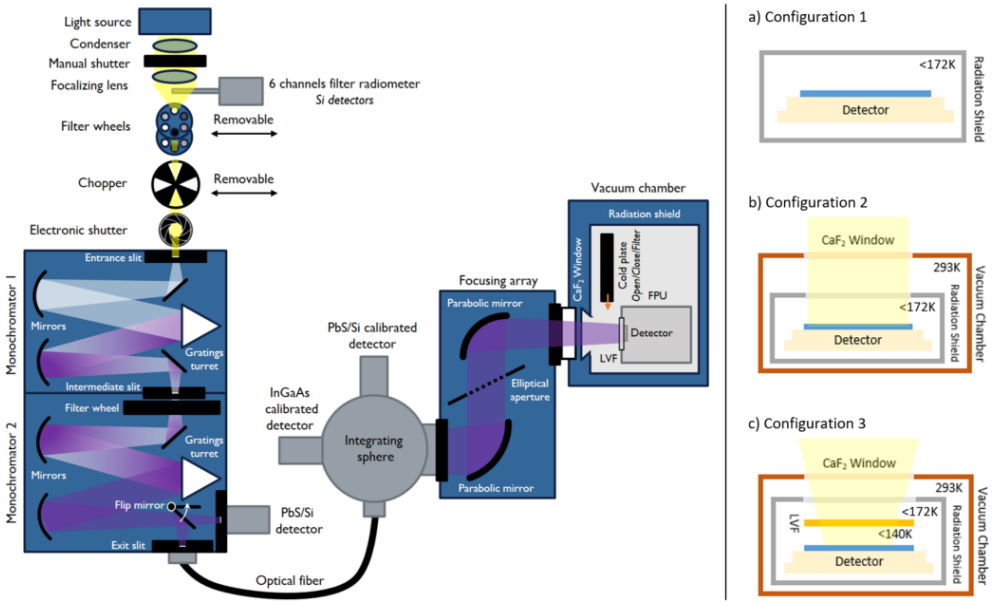

Figure 2. The optical diagram of the VIS-NIR characterization facility. In configuration 1 (a), the facility provides dark conditions by closing the movable plate inside the radiation shield. In configuration 2 (b), the output of the integrating sphere is directly connected to the viewport of the vacuum chamber to provide a uniform light beam to the detector; there is no LVF in front of the FPA for this configuration. In configuration 3 (c), the facility simulates the MAJIS collimating optics to characterize the FPU with the LVF.

on the purpose of the measurement and the wavelength to be explored. The Optical Ground Support Equipment (OGSE) system is in charge of the remote control of the optical bench of the characterization facility and, additionally, it can be synchronized with the FPU-GSE to perform quasi-automated measurements. Figure 2 shows the optical diagram of the characterization facility and a simplification of the three configurations, as they should be perceived by the detector.

3. DETECTOR INTEGRATION AND OPTICAL ALIGNMENT

The VIS-NIR H1RG detector of MAJIS is a 1024 x 1024 pixel array. The size of one pixel is 18 μm per side, and it will be binned two by two for the MAJIS mission[7]. However, the laboratory characterization must be performed for each individual pixel of the detector. Although a precise and reproducible optical alignment of the FPU is not usually necessary for characterization campaigns, the need to perform calibrated measurements such as QE and useful spectral range, demands an absolute calibration in the FPA plane of the characterization facility. For this purpose, a radiometric characterization of the FPA plane in the facility was performed,[9] by defining the optical axis of the facility as the orthogonal and centered path on the viewport of the vacuum chamber. In this way, it is possible to know the total optical power that reaches every individual pixel of the FPA for a selected wavelength and bandpass of the monochromatic illumination provided.

To guarantee the consistency between the real mount and the optomechanical design, the FPU mount was assembled by using screws with conical heads and a calibrated torquemeter. In this way, the three degrees of freedom considered in rotation were mechanically solved by the mount itself, and only the three degrees of freedom considered in translation were adjusted during the alignment procedure. The alignment procedure of the MAJIS VIS-NIR FPU was mechanically performed by using jigs and it was validated in precision and repeatibility by a laser aligned to the optical axis of the facility before the MAJIS VIS-NIR FM detector delivery.

The integration of the MAJIS VIS-NIR FM detector in the characterization facility took place in an ISO-5 area with a controlled environment in terms of temperature (22 $\pm$ 3 °C), relative humidity (45 % - 65 %) and pressure (900 mbar - 1080 mbar)[7]. After the unpacking of the FM detector, a visual inspection of the state of

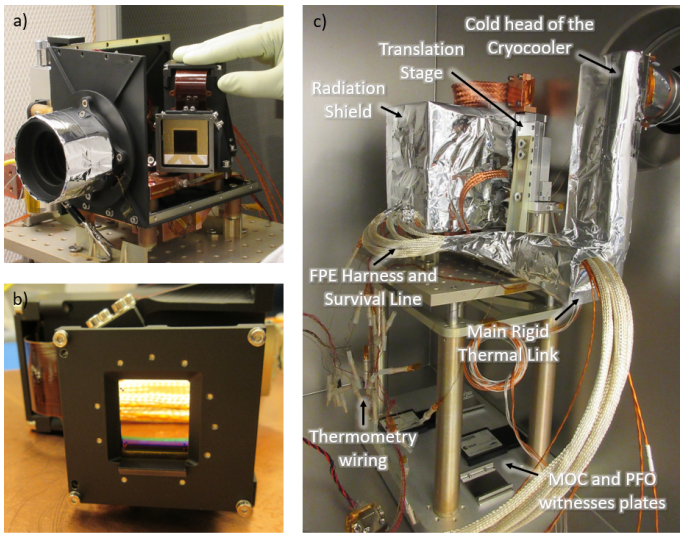

Figure 3. MAJIS VIS-NIR FM FPU integration to the characterization facility at BIRA-IASB: a) integration of the FPU without LVF inside the radiation shield, b) visual inspection of the FPU with LVF after unpacking , c) final view of the FPU mount inside the vacuum chamber with the FM FPU already installed.

the FPU was performed, followed by some functional tests at room conditions. Figure 3 shows some pictures of the FM FPU integration during both campaigns and the final view of the FPU mount before the closing of the chamber. Molecular Organic Contamination (MOC) and Particle Fall-Out (PFO) witnesses plates were used during the campaign to measure the cleanliness conditions at which the detector was exposed.

After the successful integration of the FPU mount in the vacuum chamber, additional functional tests of the FPU, the thermal control loops of the FPU mount and the translation stage, were performed before the pumping-down of the vacuum chamber. This was also the case before starting the cooling-down process (functional tests under high-vacuum environment).

4. CHARACTERIZATION CAMPAIGNS

As previously mentioned, the characterization of the MAJIS VIS-NIR FM detector was divided in two parts: FPU without LVF, and FPU with LVF as it will be in its final configuration in the spacecraft. No information is provided in this paper concerning the SM detector since it will be characterized after the time of meeting.

Before each characterization campaign, a pre-campaign of measurements was performed to: characterize the temperature differences between the FPA and the copper base plate, adjust the bias level for frame acquisition, quantify the straylight present in the detector, verify the optical alignment performed, adjust the fluxes and integration times that will be used during the measurements, characterize the thermal behavior of the FPU while operating at different acquisition modes, and verify the synchronization between the closing of the electronic shutter and the image acquisition for latency measurements[10]. Additionally during the campaigns, a quasi-real-time data processing was performed to verify if criteria of success were met for each measurement.

4.1 Characterization without the Linear Variable Filter

The measurement plan of the characterization campaign of the FPU without the Linear Variable Filter (LVF) installed, included the use of the optical configurations 1 and 2 of the facility. Moreover, the temperature exploration of the FPA temperature was limited to four values: 125 K, 132 K (nominal temperature), 140 K, and 144 K. The measurement plan performed is summarized in Figure 4, although it underwent many changes following the results of the quasi-real-time data processing performed during the campaign.

The FPU was firstly thermalized at 132 K in the FPA and it took 6.5 hours to stabilize from the activation of the cryocooler at room temperature. After 6 days of measurements, the temperature of the FPA was set to

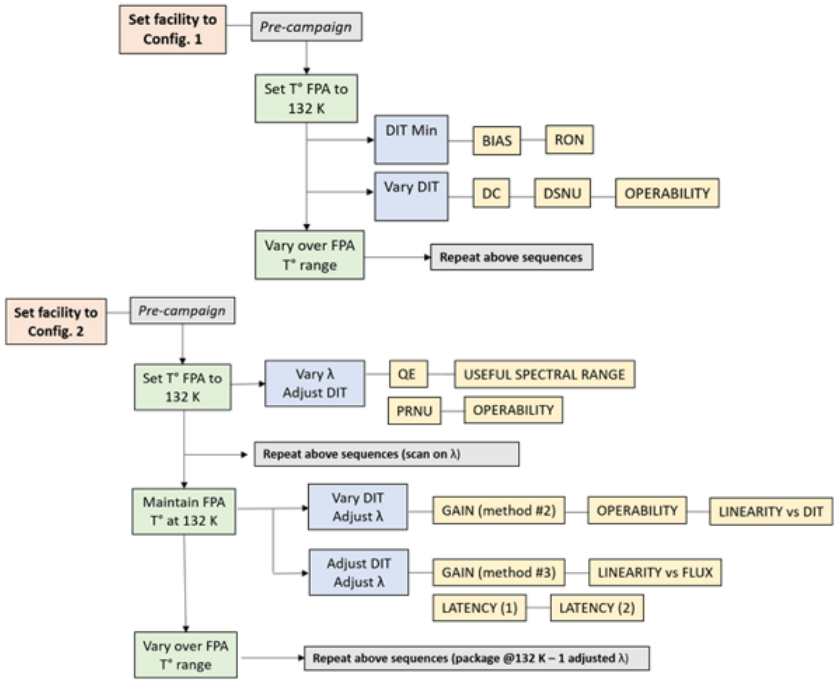

Figure 4. Measurement flow for the MAJIS VIS-NIR FM FPU characterization without LVF.[10]

125 K for characterization measurements with lower dark current. The hot case (FPA temperature at 144 K) was later explored during 2 days. For the last day of the campaign, the temperature of the FPA was fixed to 140 K. During this campaign, 15 min were required to increase the temperature of the FPA by 1 K, and 5 min to decrease it by 1 K. Moreover, at least 2 hours in addition were required for the complete thermal stabilization of the FPU before performing any characterization measurement; the temperature of the FPA is considered as stable when it does not exceed ± 0.5 K from the target temperature in at least one hour. As expected,[6] the vacuum chamber kept a stable vacuum level of 10^{-7} mbar along the campaign.

It is worth to mention that during the validation tests of the facility,[6] it was noted that the temperature of the FPU can be perturbed by the different positions of the movable plate (CLOSE, SWPF and OPEN) due to the incoming light beam inside the radiation shield. These perturbations are compensated at the base plate level thanks to its temperature control loops. Nevertheless, the FPA could increase its temperature despite the stability of the copper base plate which could drive the FPA outside its temperature of characterization. Similarly but in a stronger way, the temperature of the FPA is inevitably perturbed by the increasing temperature of the FPE during image acquisition, as it is shown by Figure 5. For this campaign, it was decided to compensate these temperature variations by regulating the temperature at the copper base plate in real-time. Unfortunately, the response of the heaters in the copper base plate induced parasite straylight in the detector due to a lack of shielding. The VIS-NIR facility could not be validated for dark measurements during the pre-campaign due to the inhomogeneity of the straylight that could not be characterized. Other potential sources of straylight found were the slit in the radiation shield through which the translation stage supports the movable plate, the slit at the rear part of the radiation shield through which the FPE harnesses and thermometry wiring pass out, and the hole at the bottom of the radiation shield through which the rigid thermal link is in contact with the copper base plate. None of these potential sources of straylight were observed during the validation tests made before the delivery of the FM detector. In consequence, all dark measurements were cancelled for this campaign and some light measurements had to be repeated without thermal compensation at the copper base plate. The cancelled measurements included Dark Current (DC) and Dark Signal Non-Uniformity (DSNU); Read-Out Noise (RON) was estimated from background measurements.

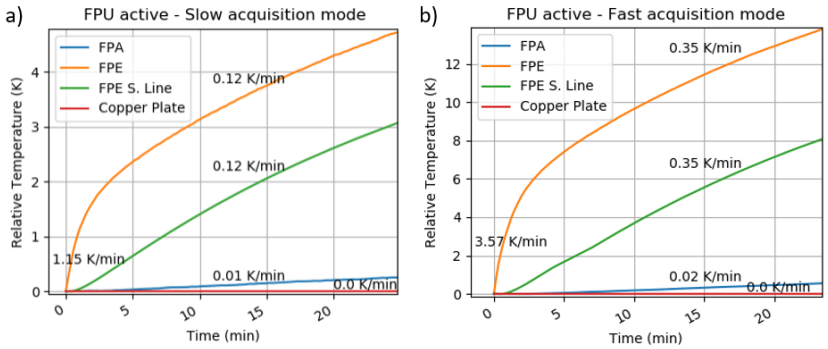

Figure 5. Thermal influence of the FPE (orange) over the FPA (blue) during two different frame acquisition speeds. The test was performed when the FPA was thermalized at 132 K. The estimated amplification factor, that could be defined as the ratio between FPA and FPE temperature increase, is roughly around 10 in the slow acquisition mode, and 13 in the fast acquisition mode. Note that at the beginning of the acquisition, the temperature increase ratio of the FPE is approximately 10 times larger than 5 min later. The FPA would achieve a temperature outside its operating temperature ($\pm$ 0.5 K) after 50 minutes in the slow acquisition mode but after 20 min in the fast acquisition mode. The offset observed between the temperature at the FPE (orange) and its survival line (green) is because of the location of their temperature sensors: the FPE sensor is located at the electronics itself, while the survival line sensors are on its surface.

4.2 Characterization with the Linear Variable Filter

The second part of the characterization campaign of the MAJIS VIS-NIR FM detector included the use of the optical configuration 3 of the facility and the Linear Variable Filter (LVF) installed in the FPU. In this configuration, the focusing array is aligned in front of the viewport of the vacuum chamber and the integrating sphere is aligned in front of the focusing array of the facility, so a uniform light beam with a convergence of 11° can be provided to the LVF-FPA[6]. This time, the temperature exploration of the FPA was limited to 132 K (nominal temperature) and 144 K (hot case). The measurement plan is summarized in Figure 6, although similarly to the previous campaign, it was optimized by following the results of the quasi-real-time data processing of the images.

Again, the FPU was firstly thermalized at 132 K in the FPA with the same rate of change (-0.7 K/min). For this campaign, the warm-up procedure was modified to optimize the total waiting time. In this way, to increase the temperature of the FPA by 1 K only 3 minutes were needed, which is about 5 times faster than during the

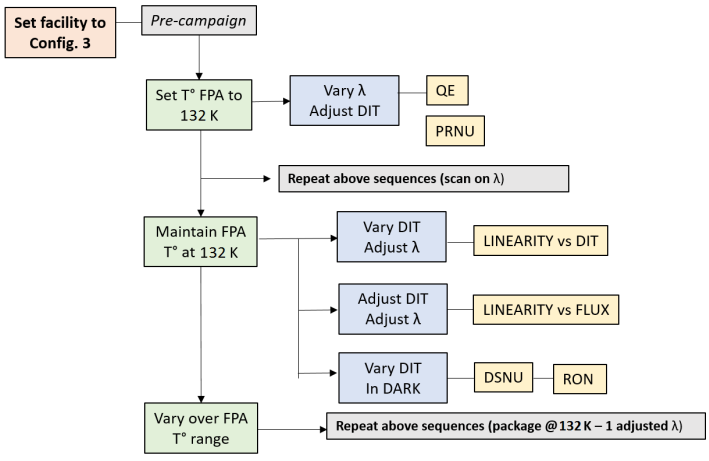

Figure 6. Measurement flow for the MAJIS VIS-NIR FM FPU characterization with LVF.[10]

previous campaign. Decreasing the temperature of the FPA by 1 K was still limited to 5 minutes. On the other hand, the vacuum and temperature evolution observed was pretty similar to the previous campaign except by the temperature of stabilization of the movable plate. To solve the straylight issue found during the first part of the characterization campaign, the FPU mount was slightly modified to improve the shielding of the identified elements that might be producing straylight. The improvements related to the shielding of the movable plate allowed to reduce its temperature by 9 K more, achieving a temperature of 148 K in closed position.

In order to reduce the risk of straylight during the measurements, it was decided to avoid temperature compensation in real-time in the copper base plate (even if the heaters were shielded now). Therefore during the pre-campaign, the movable plate was set to its different positions to characterize the thermal influence of its different states on the FPA temperature. In this way, a temperature compensation could be performed before image acquisition in a new configuration. Figure 7 shows the thermal response observed in the FPA and the movable plate depending on the positions of the movable plate. The temperature changes are simultaneous because both elements are directly affected by the incoming light inside the radiation shield at the same time. Note that the temperature of the FPE does not change considerably; along the whole test, the FPE increased its temperature by no more than 1 K while inactive. Actually, the thermal influence of the FPE over the FPA was not compensated during this campaign neither. Instead, the FPA temperature was thermalized 0.5 K below the target temperature[10] to provide about 1 K margin during the measurements, while meeting the temperature requirements ($\pm$ 0.5 K)[7]. As it was the case for the previous campaign, the temperature of the FPA and the FPE was continuously inspected during the measurements, especially the temperature of the FPE, that must remain below 160 K to avoid additional noise in the images.

The campaign was mainly focused on the verification of the LVF alignment (within 300 μm of error[7] and measured with a precision of about 200 μm). Additional tests were performed during the campaign, mainly the simulation of a typical MAJIS GCO-5000 segment observation. Moreover during the campaign, it was possible to perform a fine scanning over the VIS-NIR spectral range (instead of 20 pre-selected wavelengths[6]) and linearity measurements. Thanks to the improvements performed to avoid straylight on the detector, measurements in dark conditions were also performed. The survival line of the FPU was successfully tested.

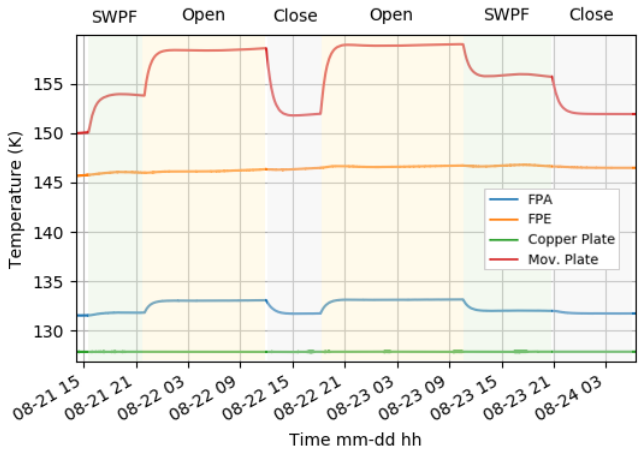

Figure 7. Thermal impact of the different positions of the movable plate over the FPA. The FPA (blue) was thermalized at 132 K and the FPE (orange) was inactive during the test. The thermal perturbations induced in the copper plate (green) were compensated by its PID temperature control loops. The movable plate (red) could increase its temperature by 7.4 K when passing from close to open position, but since it was still below the temperature limit of 172 K, its thermal emission was negligible for the FPA. To compensate the observed differences, the temperature of the copper plate (and consequently the temperature of the FPA) was decreased by 1.4 K when opening the radiation shield and by 0.2 K when using the SWPF. For dark measurements, the copper plate kept a temperature of 3.8 K below the target temperature of the FPA[10]. Although it is not shown, the temperature of the radiation shield was less affected: for the coldest case, it remained about 10 K above the temperature of the copper plate.

5. PRELIMINARY RESULTS

During the campaigns, a quasi-real-time data processing was performed to verify if criteria of success were met for each measurement. A software package based on Photon Transfer Curve (PTC) methodology, previously used for the characterization of the CMOS detector of the Extreme Ultraviolet Imager (EUI) of the Solar Orbiter mission,[11] was adapted to the H1RG images from the MAJIS detector to be used for a cross check analysis of the data during the post-processing phase. This section describes the preliminary results obtained after each campaign of measurements without including the data analysis developed through the PTC methodology, which is still under development. The radiometric, thermometry and environmental data obtained during the characterization campaign, was also analyzed in case of further details are needed about the conditions at which the measurements were made. Table 1 summarizes the measurements performed during the campaign and the different conditions under they were characterized.

Table 1. Measurements performed during the MAJIS VIS-NIR FM FPU characterization campaign. The preliminary results obtained are compatible with the specifications[12]. However, further analysis need to be performed before providing the final performances of the detector.

Parameter	**Temperatures [K]**	**Total # DIT**	**Wavelengths [nm]**	**# I. Levels**	**Read-Out Modes**	**Preliminary Results** [a]
DC and DSNU	132	2	N/A	N/A	Slow	< 2500 e^-/s
	144	13	N/A	N/A	Slow	
QE and Spectral Range	125, 144	1	800	1	Both	TBE
	132	1	425 - 2550	1	Both	
	140	1	800, 2450 - 2600	1	Both	
Linearity vs DIT	125, 132, 144	40	545	1	Both	5 %
Linearity vs Flux	125, 132, 144	1	910 or 1080 [b]	30	Both	5 %
	132, 144	1	910, 1160	30	Slow	
Operability and pixels mapping	125, 144	45	800	1	Both	TBE
	132	45	425 - 2550	1	Both	
	140	1	800, 2450 - 2600	1	Both	
PRNU	125, 144	1	800	1	Both	TBE
	132	1	425 - 2550	1	Both	
	140	1	800, 2450 - 2600	1	Both	
Bias & Straylight	125 - 144	4	545	1	Both	TBE
	132 [c]	15	N/A	N/A	Slow	
Latency	132	1	1080	1	Fast	< 3 %
Conversion Gain	125, 132, 144	41	545, 910, 1080	31	Both	TBE
	140	3	545	1	Both	
LVF alignment	132, 144	1	480 - 2350	1	Both	< 300 μm

[a] At operative temperature.
[b] Depending on the read-out mode used.
[c] Performed during the campaign with LVF.

As previously stated, DC and DSNU had to be canceled due to the high level of straylight found on the detector during the first campaign of measurements. However, the Read-Out Noise (RON) was estimated from the bias and straylight measurements performed in dark conditions. Moreover, thanks to the large improvements on the shielding of the FPU mount for the second campaign of measurements, the optical configuration 1 for dark measurements was rehabilitated and the frames obtained were very close to the expected dark level values

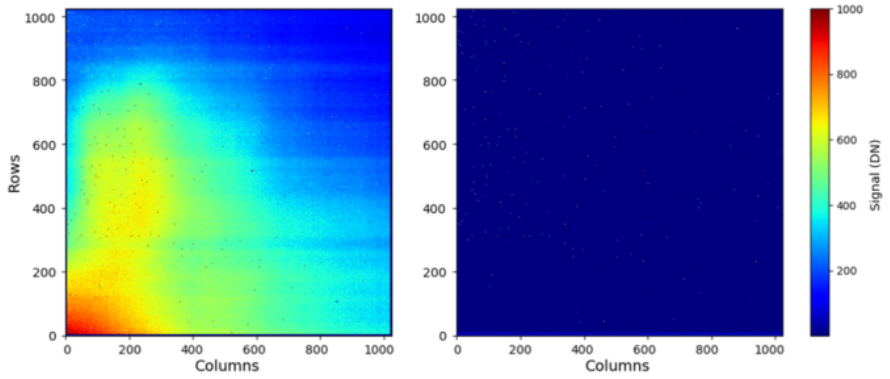

Figure 8. Dark images of the MAJIS VIS-NIR FM detector during the characterization campaign to visualize the level of straylight in the detector. The level of straylight observed during the first part of the characterization campaign (left) was high enough to cancel dark measurements. Neverhteless, the setup was improved to reduce the level of straylight for the second part of the campaign (right), corresponding to the characterization of the detector in its final configuration, and the dark measurements were successfully performed.

(below 2500 e^-/s). Figure 8 compares dark images acquired before and after the shielding improvements, where the level of straylight is clearly observed. The background measurements performed with the movable cold plate in SWPF position, confirm a low and very homogeneous residual FPA illumination. Although some residual straylight is still observed in the preliminary results, the bottom rows of the detector offer the possibility to estimate the upper limits of DC.

The study of QE, Photo-Response Non-Uniformity (PRNU) and operability is not yet completed since information about the optical power provided by the facility, for wavelengths above 1220 nm, is still missing[6]. Further analysis need to be performed before providing the measured information.

The linearity is defined as the deviation of the detector response for each operable pixel. The linear range will correspond to the fraction of well depth over which the photometric response is within 5 % of the mean slope. When the deviation exceeds 5 % of the local expected value, this value will correspond to the Full Well Capacity (FWC)[7]. Concerning the linearity of the detector response measured versus different Detector Integration Time (DIT) values and different dynamical illumination levels, the typical result is a 5 % deviation occurring above 50000 e^- in both acquisition modes. Moreover, it was observed that the temperature of the FPA has only a minor effect in its linearity. Figure 9 and Figure 10 show examples of results from linearity measurements for both acquisition modes. Note that due to the different memory storage formats corresponding to the each acquisition

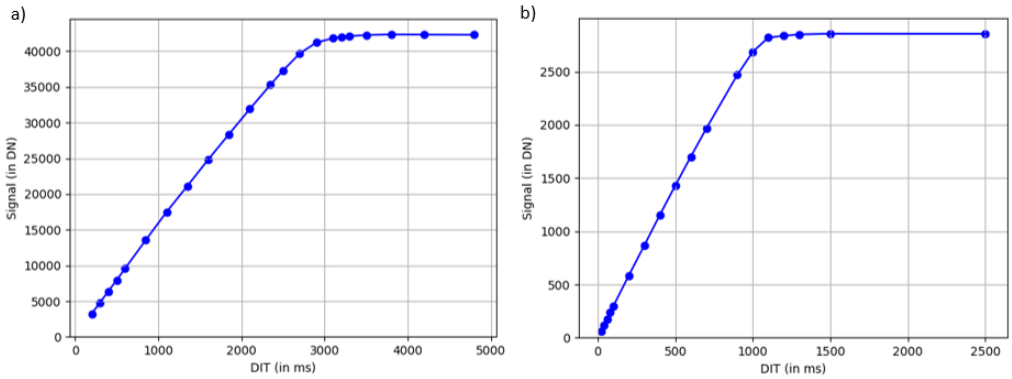

Figure 9. Example of results from linearity measurements vs DIT performed during the characterization campaign without LVF (FPA at 125 K): a) Image acquisition in slow mode, b) Image acquisition in fast mode.

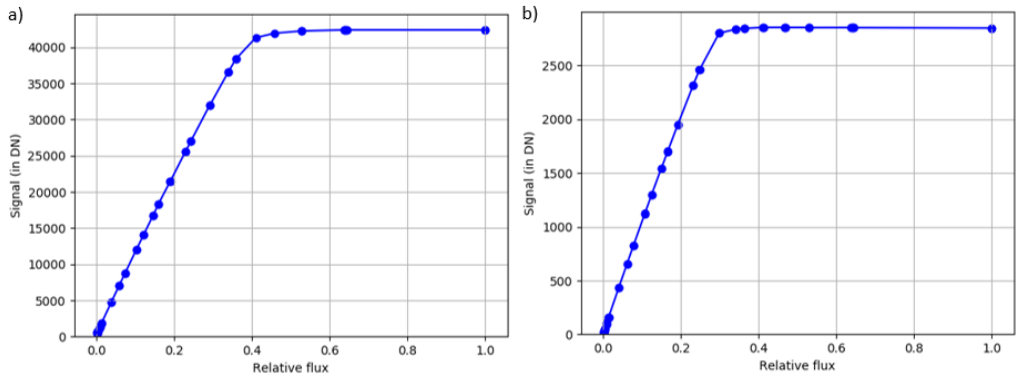

Figure 10. Example of results from linearity measurements vs flux performed during the characterization campaign without LVF (FPA at 125 K): a) Image acquisition in slow mode, b) Image acquisition in fast mode.

mode, there is a factor about 16 between both acquisition modes for each case.

The latency or persistence of the detector, which corresponds to the amount of residual photocharge left in a pixel from previous readouts, was measured by closing the electronic shutter at the entrance of the monochromator with the movable plate in SWPF position. In this way, the blackbody emission at NIR wavelengths coming from the viewport of the vacuum chamber and beyond is reduced. The difficulty of this procedure lay in the synchronization between the closing of the shutter (23 ms)[13] and the image acquisition. The latency was estimated to be less than 3 %, which is in accordance with the detector specifications[12].

The LVF was accurately integrated at IAS facilities and aligned by using a microscope by the end of July 2020. The alignment was verified during the characterization campaign at BIRA-IASB by using frame acquisitions. Because of the possibility to observe the shadow of the fiducial markers on the FPA, it was possible to verify the alignment of the LVF by three different methods. Following the center position of the LVF, the larger wavelength for which a cut-on is observable on a frame under monochromatic illumination was verified to be around 1650 nm. On the other hand, since the fiducial markers were visible in the top-left, top-right and bottom-left corners of a frame (Figure 11), two fiducial markers could be seen in the SWPF position (cut-off at 1.5 μm) in slow acquisition mode, and the three in open position and fast mode. Windowing technique was used for the last mentioned method to reduce the risk of saturation of the detector from room temperature emitters. The position of the center of the LVF with respect to the center of the FPA, meets the maximum misalignment requirement of 300 μm for the spectral dimension with respect to the theoretical position[7], and was fully confirmed by the three applied methods. It is worth mentioning that the transmission of the LVF can be determined by modeling

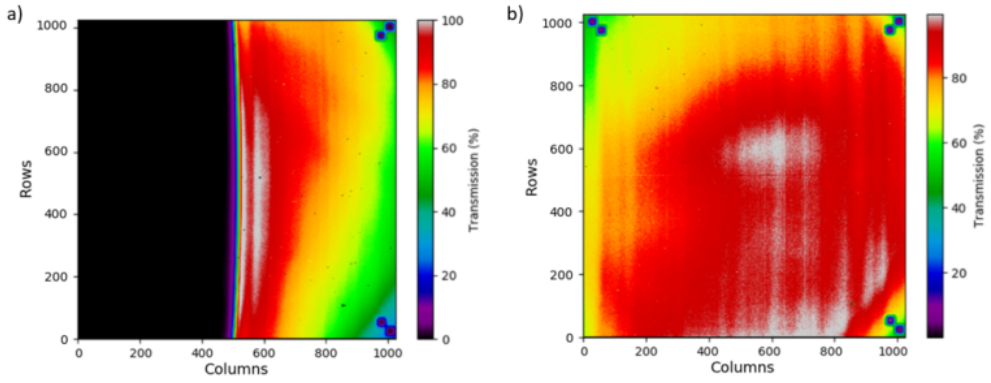

Figure 11. Example of acquisitions under monochromatic illumination to verify the alignment of the LVF with respect to the FPA: a) 1020 nm to visualize two fiducial markers, b) 1765 nm to visualize the three fiducial markers.[10].

the reference signal of the FPA plane without LVF in the optical configuration 3 of the facility, with a post-processing of the data from the first campaign[10]. As previously mentioned, the lamp signal has been monitored by the photodiodes in the integrating sphere during the campaign, and the homogeneity in the FPA plane as well as the difference in optical power between the integrating sphere and the FPA plane, is well characterized for configurations 2 and 3.

Simulation of the MAJIS GCO-5000 segment observation

One additional measurement performed when the FPU was assembled in its final configuration with the LVF, was the simulation of a GCO-5000 segment observation. Two phases in circular orbit around Ganymede are foreseen during the mission: at an altitude of 5000 km with an expected duration of 80 terrestrial days, and at an altitude of 500 km during 133 terrestrial days[14]. These phases can be referred to as Ganymede Circular Orbit - 5000 (GCO-5000) and GCO-500, respectively. The GCO-5000 phase will contribute to the global imaging and spectro-imaging of Ganymede, to study its geology and surface composition, taking advantage of good illumination conditions, since the angle between the JUICE orbital plane and the Ganymede-Sun vector shall be between 20° and 30°.[15]

The simulation of the GCO-5000 segment observation took place when the FPA was thermalized at 132 K. The test consisted in simulate a typical data acquisition for the MAJIS VIS-NIR channel in this orbital phase (fast acquisition mode), in order to observe the thermal performances of the FPU and technically confirm the possibility to proceed with these sequences. The image was acquired in dark conditions (facility in configuration 1). The complete test lasted about 90 minutes. Figure 12 shows the results observed and the temperature ratio for each curve considering a linear approximation. Note that the behavior of the FPE is pretty similar to the observed in Figure 5, although the slope decreases after the first 30 minutes and seems to achieve stabilization some minutes later. When the FPE is not longer in operation, its temperature decreases roughly by 1 K/min during the first 2 minutes, and later by 0.3 K/min. The results of this simulation validated the observational strategy planned for MAJIS along the mission.

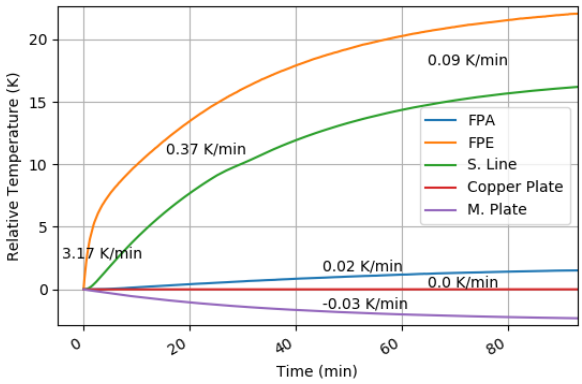

Figure 12. Thermal influence of the FPE (orange) over the FPA (blue) during the simulation of the MAJIS GCO-5000 segment observation. The test was performed when the FPA was thermalized at 132 K with the FPE operating in fast acquisition mode. The maximum temperature achieved by the FPE during the test was 171 K. Note that after 30 min of operation the temperature of the FPE increases with a lower rate that might stabilize. Therefore, the estimated amplification factor defined as the ratio between FPA and FPE temperature increase, is roughly around 13, during the first 30 min of the test, and around 10 after starting to stabilize. Nevertheless, the movable plate (purple) was changed from OPEN to CLOSE position during the test, so it is possible that the temperature of the FPA was lower than expected.

6. CONCLUSIONS

During the two weeks devoted to the MAJIS VIS-NIR FM characterization campaign without the LVF, different tests were performed in order to measure the RON, QE, PRNU, operability, linearity, latency and conversion gain of the detector. The second part of the campaign consisted in the characterization of the FM in its final configuration (with LVF) by providing a uniform light beam with the same convergence that the detector

will receive in MAJIS. The tests performed during the six days devoted to the last campaign, included the GCO-5000 segment simulation, the LVF alignment verification, dark measurements and linearity measurements; the functioning of the survival line of the FPU was also verified.

The FPA was thermalized at different temperatures: 125 K, 132 K (nominal temperature), 140 K and 144 K (expected hottest case). The performances of the thermal regulation of the VIS-NIR facility were nominal and the temperature of the FPA remained within its stabilization range (target temperature $\pm$ 0.5 K). The measurements were always performed while the temperature of the FPE was below 160 K to avoid additional noise in the images. The thermal influence of the FPE over the FPA was well characterized for the different read-out modes of the detector and were not compensated mainly during the second part of the characterization campaign. Nevertheless, some thermal compensations were performed to reduce the impact of the incoming light beam on the temperature of the FPU when the movable plate in front of the detector was changed to a different position (CLOSE, SWPF or OPEN), in order to keep the FPA temperature within its expected range.

The simulation of a typical MAJIS VIS-NIR observation was successfully performed during the second part of the characterization campaign to validate the observational strategy planned for MAJIS along the mission. This simulation demonstrated that the GCO-5000 sequence is technically possible from a thermal point of view. Although the FPE influences the stability of the temperature of the FPA, while in operation, the FPA roughly increases its temperature by 0.02 K/min. Therefore, it is expected that the temperature of the FPA increases by 1 K only after 50 min of measurements. On the other hand, since normally the temperature of the FPE is 13 K above the temperature of the FPA (FPE non-operating), the FPE would achieve a temperature of 160 K after 25 minutes in operation, which is the maximum recommended temperature to acquire images with the minimal noise from the FPE.

Although the measurements were disturbed by the unexpected level of straylight on the detector during the first campaign, the characterization was considered compliant with the defined criteria of success. However, the facility was improved in order to reduce the level of straylight before the delivery of the FM in its final configuration. The dark conditions provided to the detector had significantly improved, and the background radiation remained low and homogeneous during measurements. In consequence, the dark measurements were successfully performed during the last campaign and the preliminary results obtained provided an estimation of the upper limit of the DC of the detector.

The VIS-NIR characterization facility developed is ready for the MAJIS VIS-NIR SM campaign, which is planned by mid-January 2021.

ACKNOWLEDGMENTS

This project acknowledges funding by the Belgian Science Policy Office (BELSPO) by PRODEX-11 Project Proposal: *Characterization of JUICE/MAJIS VIS-NIR detectors* (PEA 4000124255), as well as by the Scientific Research Fund (FNRS) by the Aspirant Grant: 34828772 *MAJIS detectors and impact on science*. Additional funding is provided since end of 2019 by the ESA JUICE Project.

REFERENCES

[1] Grasset, O., Dougherty, M., Coustenis, A., Bunce, E., Erd, C., Titov, D., Blanc, M., Coates, A., Drossart, P., Fletcher, L. N., et al., "JUpiter ICy moons Explorer (JUICE): An ESA mission to orbit Ganymede and to characterise the Jupiter system," *Planetary and Space Science* **78**, 1–21 (2013).

[2] Langevin, Y., Piccioni, G., and team, M., "MAJIS (Moons and Jupiter imaging spectrometer) for JUICE: objectives for the galilean satellites," in [*European Planetary Science Congress*], **8**, 548–1 (2013).

[3] Guiot, P., Vincendon, M., Carter, J., Lecomte, B., Poulet, F., Lami, P., and Langevin, Y., "JUICE/MAJIS on-ground calibration: challenges and setup design.," in [*Geophysical Research Abstracts*], **21** (2019).

[4] Langevin, Y., Pascal, E., Renotte, E., Gérard, J.-C., Karatekin, Ö., and Ann-Carine, V., "Memorandum of Understanding between IAS and CSL, ULiège, ROB and BIRA-IASB." 2015.

[5] Bolsée, D., Van Laeken, L., Cisneros-González, M. E., and Pereira, N., "MAJIS VIS-NIR Characterization. Team organization and responsabilities," tech. rep., Royal Belgian Institute for Space Aeronomy (BIRA-IASB) (2020). Ref: IASB-MAJ-TN-011-2.1.

[6] Bolsée, D., Van Laeken, L., Cisneros-González, M. E., Pereira, N., Depiesse, C., Jacobs, L., Vandaele, A. C., Ritter, B., Gissot, S., Karatekin, Ö., et al., "Characterization facility for the MAJIS/JUICE VIS-NIR FM and SM detectors," in [*Space Telescopes and Instrumentation 2020: Optical, Infrared, and Millimeter Wave*], **submitted**, International Society for Optics and Photonics (2020).

[7] MAJIS Team, "MAJIS FPU VIS-NIR Requirement Specifications," tech. rep., Institute of Space Astrophysics (IAS) (2018). Ref: JUI-IAS-MAJ-RS-021.

[8] Cisneros-González, M. E., Bolsée, D., Van Laeken, L., Pereira, N., Pierre, G., Vandaele, A. C., Karatekin, Ö., Poulet, F., Dumesnil, C., Dubois, J. P., et al., "Thermal-vacuum and security system of the characterization facility for MAJIS/JUICE VIS-NIR FM and SM detectors," in [*Space Telescopes and Instrumentation 2020: Optical, Infrared, and Millimeter Wave*], **submitted**, International Society for Optics and Photonics (2020).

[9] Van Laeken, L., *Development of experimental benches for radiometric characterization: Application to space instrument MAJIS VIS-NIR on JUICE.*, Master's thesis, Université de Liège, Liège, Belgium (2019).

[10] Bolsée, D., Van Laeken, L., Cisneros-González, M. E., , Pereira, N., and Haffoud, P., "MAJIS VIS-NIR Characterization FM campaign," tech. rep., Royal Belgian Institute for Space Aeronomy (BIRA-IASB) (2020). Ref: IASB-MAJ-VR-010-2.2.

[11] BenMoussa, A., Giordanengo, B., Gissot, S., Meynants, G., Wang, X., Wolfs, B., Bogaerts, J., Schühle, U., Berger, G., Gottwald, A., et al., "Characterization of backside-illuminated CMOS APS prototypes for the Extreme Ultraviolet Imager on-board Solar Orbiter," *IEEE transactions on electron devices* **60**(5), 1701–1708 (2013).

[12] Teledyne Imaging Sensors, *H1RG^{TM} Visible and Infrared Focal Plane Array* (2018).

[13] Uniblitz, *DSS35B Bi-stable Optical Shutter* (2016).

[14] Ortore, E., Circi, C., and Cinelli, M., "Optimal orbits around Ganymede for the JUICE mission," *Aerospace Science and Technology* **46**, 282–286 (2015).

[15] ESA, [*JUICE: Exploring the emergence of habitable worlds around gas giants. Definition Study Report*], ESA (2014).

APPENDIX A. ACRONYMS

BIRA-IASB	Royal Belgian Institute for Space Aeronomy
BUSOC	Belgian User Support and Operations Center
CDS	Correlated Double Sampling
CMOS	Complementary Metal–Oxide–Semiconductor
CNES	National Centre for Space Studies
DC	Dark Current
DIT	Detector Integration Time
DN	Digital Number
DSNU	Dark Signal Non-Uniformity
EUI	Extreme Ultraviolet Imager
ESA	European Space Agency
FM	Flight Model
FNRS	Scientific Research Fund
FPA	Focal Plane Array
FPE	Focal Plane Electronics
FPU	Focal Plane Unit
FWC	Full-Well Capacity
GCO	Ganymede Circular Orbit
GSE	Ground Support Equipment

IAS	Institute of Space Astrophysics
IR	InfraRed wavelength range
ISO	International Organization for Standardization
JUICE	JUpiter Icy Moons Explorer
LVF	Linear Variable Filter
MAJIS	Moons And Jupiter Imaging Spectrometer
MOC	Molecular Organic Contamination
NIR	Near-InfraRed wavelength range
OGSE	Optics Ground Support Equipment
PA	Product Assurance
PFO	Particle Fall-Out
PID	Proportional-Integral-Derivative
PRNU	Photo-Response Non-Uniformity
PTC	Photon Transfer Curve
QA	Quality Assurance
QE	Quantum Efficiency
ROB	Royal Observatory of Belgium
RON	Read-Out Noise
SM	Spare Model
SWPF	Short-Wave Pass Filter
TBE	To Be Evaluated
TGSE	Thermal Ground Support Equipment
VIS	VISible wavelength range